HEAVY MESON COHERENT PHOTOPRODUCTION IN (ULTRA)-PERIPHERAL *AA* COLLISIONS*

M.B. Gay Ducati, S. Martins

High Energy Physics Phenomenology Group, GFPAE IF-UFRGS
Caixa Postal 15051, CEP 91501-970, Porto Alegre, RS, Brazil

(Received March 5, 2019)

The exclusive photoproduction of the J/ψ state is investigated in peripheral AA collisions for the energies available at the LHC, $\sqrt{s} = 2.76\,\text{TeV}$ and $\sqrt{s} = 5.02\,\text{TeV}$, in different centrality classes. The rapidity distribution and the nuclear modification factor (R_{AA}) were calculated from the light-cone color dipole formalism. Three scenarios were considered: (1) a similar formalism adopted in the UPC regime is used, (2) one considers that only the spectators in the target are the ones that interact coherently with the photon, and (3) the photonuclear cross section is modified using the same geometrical constraints applied in scenario 2. The results were compared with the ALICE measurements (only J/ψ at the moment) and show a better agreement in the more complete approach (scenario 3), mainly in the more central regions (30%–50% and 50%–70%) where the dependence on b is deeper.

DOI:10.5506/APhysPolBSupp.12.819

1. Introduction

The ALICE Collaboration measured the J/ψ hadroproduction in peripheral collisions Pb–Pb, with $\sqrt{s} = 2.76\,\text{TeV}$, revealing an excess in the production of the meson in very small transverse momentum ($p_{\text{T}} < 0.3\,\text{GeV}/c$) in the range rapidity of $2.5 < y < 4.0$ [1]. This excess was also measured by the STAR Collaboration for 20%–40%, 40%–60% and 60%–80% centrality classes at $\sqrt{s} = 200\,\text{TeV}$ (Au–Au) and $\sqrt{s} = 193\,\text{GeV}$ (U–U). In our approach, this excess is investigated from the exclusive photoproduction mechanism, considering three scenarios: (1) a photon flux with b-dependence was used, (2) a geometrical cut is applied in the photon flux ensuring that only the spectators in the target will interact coherently with the photon,

* Presented at the Diffraction and Low-x 2018 Workshop, August 26–September 1, 2018, Reggio Calabria, Italy.

and (3) where, for completeness, the same restriction adopted in scenario 2 to construct the effective photonuclear cross section was applied. Using these three scenarios, the rapidity distribution and the nuclear modification factor, R_{AA}, were estimated for 30%–50%, 50%–70% and 70%–90% centrality classes.

To calculate the R_{AA}, the expression developed in [2] was adopted

$$R_{AA}^{hJ/\psi} = \frac{N_{AA}^{J/\psi}}{\mathrm{BR}_{J/\psi\to l^+l^-}\, N_{\mathrm{events}}\, (A\times\varepsilon)_{AA}^{J/\psi}\, \langle T_{AA}\rangle\, \sigma_{pp}^{hJ/\psi}}\,, \tag{1}$$

where the measured number of J/ψ ($N_{AA}^{J/\psi}$) is corrected for acceptance and efficiency $(\mathcal{A}\times\varepsilon)_{AA}^{J/\psi} \sim 11.31\%$ and branching ratio $\mathrm{BR}_{J/\psi\to\mu^+\mu^-} = 5.96\%$. Then, the result is normalized to the equivalent number of MB events ($N_{\mathrm{events}} \simeq 10.6\times 10^7$), defined in [2], average nuclear overlap function ($\langle T_{AA}\rangle$), calculated from [3], and proton–proton inclusive J/ψ production cross section ($\sigma_{pp}^{hJ/\psi} \sim 0.0514\ \mu$b), calculated from a parametrization detailed in [1].

2. Theoretical framework

The differential cross section in the rapidity y and impact parameter b can be written as [4]

$$\frac{\mathrm{d}^3\sigma_{AA\to AAV}}{\mathrm{d}^2b\mathrm{d}y} = \omega N(\omega,b)\sigma_{\gamma A\to VA} + (y\to -y)\,, \tag{2}$$

where $N(\omega,b)$ is a photon flux with b-dependence, $\sigma_{\gamma A\to VA}$ is the photonuclear cross section, which characterizes the photon–target interaction $\gamma A\to VA$, $\omega = \frac{1}{2}M_V\exp(y)$ is the photon energy, and M_V is the meson mass. In the peripheral collisions ($b<2R_A$), the use of the different electromagnetic form factor, $F(k^2)$, may become relevant. Therefore, the following photon flux was adopted [5]:

$$N(\omega,b) = \frac{Z^2\alpha_{\mathrm{QED}}}{\pi^2\omega}\left|\int_0^\infty \mathrm{d}k_\perp k_\perp^2\frac{F\left(k^2\right)}{k^2}J_1\left(bk_\perp\right)\right|^2\,, \tag{3}$$

where Z is the nuclear charge, $\gamma = \sqrt{s_{NN}}/(2m_{\mathrm{proton}})$ is the Lorentz factor, $k_\perp$ is the transverse momentum of the photon, $k^2 = (\omega/\gamma)^2 + k_\perp^2$, and the form factor for lead nucleus is given by [6]

$$F(k) = \frac{4\pi\rho_0}{Ak^3}\left[\sin\left(kR_A\right) - kR_A\cos\left(kR_A\right)\right]\left[\frac{1}{1+a^2k^2}\right]\,, \tag{4}$$

with $a = 0.7$ fm and $\rho_0 = 0.1385\ \mathrm{fm}^{-3}$.

In addition, the photonuclear cross section $\sigma_{\gamma A\to VA}$ represents the photon–nuclei interaction and is described in this work in the light cone color dipole formalism, which includes the partonic saturation phenomenon and the nuclear shadowing effects [7–9]. The formalism has already been explored in the last works [10] in pp, pA and AA collisions. In the last case, the coherent photonuclear cross section of a vector meson V can be factorized as

$$\sigma_{(\gamma A\to VA)} = \frac{|\mathrm{Im}\ A(x,t=0)|^2}{16\pi}\left(1+\beta^2(\lambda_{\mathrm{eff}})\right) R_g^2(\lambda_{\mathrm{eff}}) \int\limits_{t_{\mathrm{min}}}^{\infty} |F(t)|^2 \mathrm{d}t\,, \qquad (5)$$

where the forward scattering amplitude $A(x,t=0)$ carries the dynamical information of the process and the form factor $F(t)$ is the same as applied in (4). The parameter $\beta = \tan(\pi\lambda_{\mathrm{eff}}/2)$ restores the real contribution of the scattering amplitude and $R_g^2(\lambda_{\mathrm{eff}}) = (2^{2\lambda_{\mathrm{eff}}+3}/\sqrt{\pi})[\Gamma(\lambda_{\mathrm{eff}}+5/2)/\Gamma(\lambda_{\mathrm{eff}}+4)]$ corresponds to the ratio of off-forward-to-forward gluon distribution (skewedness effect). The parameter λ_{eff} can be estimated from the relation $\lambda_{\mathrm{eff}} \equiv \partial\ln[\mathrm{Im}\ A(x,t=0)]/[\partial\ln(1/x)]$. At last, $x = (M_V^2+Q^2)/(Q^2+2\omega\sqrt{s})$ with $Q\sim 0$ for nucleus and $t_{\mathrm{min}} = (m_V^2/2\omega\gamma)^2$. In the color dipole formalism, the photon–nuclei forward scattering amplitude is factorized in the overlap between the photon and the vector meson wave functions, and in the dipole–nuclei cross section as

$$\mathrm{Im}\ A(x,t=0) = \int \mathrm{d}^2r \int \frac{\mathrm{d}z}{4\pi} (\psi_V^*\psi_\gamma)_T\, \sigma_{\mathrm{dip}}^{\mathrm{nucleus}}(x,r)\,, \qquad (6)$$

where $(\psi_V^*\psi_\gamma)_T$ is described with more detail in [11], and $\sigma_{\mathrm{dip}}^{\mathrm{nucleus}}(x,r)$ is obtained using the Glauber–Gribov picture [12, 13], as proposed in [14]

$$\sigma_{\mathrm{dip}}^{\mathrm{nucleus}}(x,r) = 2\int \mathrm{d}^2b' \left\{1-\exp\left[-\frac{1}{2}T_A(b')\sigma_{\mathrm{dip}}^{\mathrm{proton}}(x,r)\right]\right\}. \qquad (7)$$

In Eq. (7), $T_A(b)$ is the nuclear overlap function, calculated from Woods–Saxon distribution, and σ_{dip} is the dipole–nucleon cross section, which was calculated in this work using the GBW and CGC dipole models. These two models have shown a good agreement with the data in the ultraperipheral regime [10]. The application of Eqs. (3) and (5) inside of (2) constitute what we named scenario 1.

3. The effective photon flux

To refine our calculations, an effective photon flux was built following a similar procedure showed in [4] where two hypotheses were considered:

(1) only the photons that reach the geometrical region of the nuclear target will be considered and (2) the photons that reach the overlap region will be neglected, Fig. 1. Then, the new photon flux can be expressed as [15]

$$N^{\rm eff}(\omega, b) = \int N^{\rm usual}(\omega, b_1) \frac{\theta(b_1 - R_A)\theta(R_A - b_2)}{A_{\rm eff}(b)} {\rm d}^2 b_2 \,, \tag{8}$$

where the effective interaction area, $A_{\rm eff}(b)$, is given by

$$A_{\rm eff}(b) = R_A^2 \left[\pi - 2\cos^{-1}\left(\frac{b}{2R_A}\right)\right] + \frac{b}{2}\sqrt{4R_A^2 - b^2} \,. \tag{9}$$

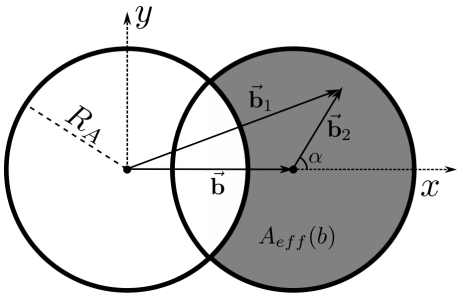

Fig. 1. Scheme of the interaction according to scenario 2.

4. The effective photonuclear cross section

In accordance with the geometrical constraints adopted in the construction of the effective photon flux, an effective photonuclear cross section was constructed applying the $\Theta\,(b_1 - R_A)$ function into Eq. (7), which produces

$$\begin{aligned} \sigma_{\rm dip}^{\rm nucleus}(x, r) \;=\; & 2 \int {\rm d}^2 b_2 \Theta(b_1 - R_A) \\ & \times \left\{1 - \exp\left[-\frac{1}{2} T_A(b_2) \sigma_{\rm dip}^{\rm proton}(x, r)\right]\right\} \,, \end{aligned} \tag{10}$$

where, $b_1^2 = b^2 + b_2^2 + 2bb_2\cos(\alpha)$. Considering the effective photon flux and photonuclear cross section, the rapidity distribution was calculated and its results for the three centrality classes (scenario 3) are shown in Table I.

5. Main results

In Table I, the average rapidity distribution using the GBW and CGC models is shown for the three scenarios described in the text.

TABLE I

Average Rapidity Distribution: $d\sigma/dy$. Comparison between our results obtained from different approximations and the ALICE data [1].

GBW/CGC	30%–50%	50%–70%	70%–90%
Scenario 1	200/170	100/84	60/51
Scenario 2	128/107	98/80	80/67
Scenario 3	73/61	78/66	75/63
ALICE data	$73 \pm 44^{+26}_{-27} \pm 10$	$58 \pm 16^{+8}_{-10} \pm 8$	$59 \pm 11^{+7}_{-10} \pm 8$

In the simplest approach (scenario 1), a good agreement with the ALICE data is reached for 70%–90% centrality class where the b-dependence is weaker. In more central regions, scenario 2 and scenario 3 are more suitable. In particular in scenario 3, one has the largest production cross section in the 50–70% centrality class. This is due to the dipole–nuclear cross section used, which is b-dependent through the $T_A(b)$ function and, therefore, it is more strongly suppressed in more central collisions due to restriction $\Theta(b_1 - R_A)$. Consequently, the 30%–50% centrality class is more affected than the 50%–70% region.

Besides the rapidity distribution, the excess of the J/ψ was also quantified by the nuclear modification factor, Eq. (1), and calculated from the results presented in Table I. Adopting the CGC model, which shows slightly better results than the GBW model, the R_{AA} was calculated for the three scenarios investigated and its results are compared with the ALICE data, Fig. 2. Similarly to the rapidity distribution, scenario 1 shows better agree-

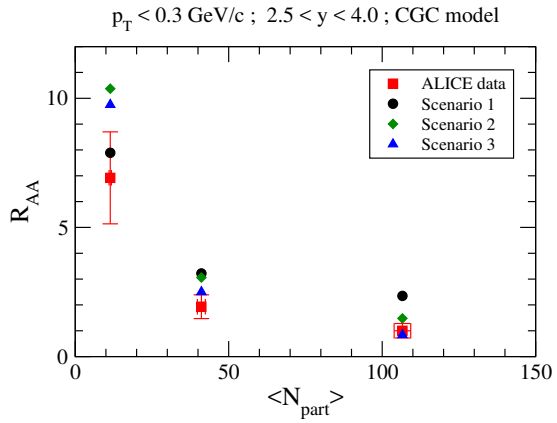

Fig. 2. Comparison of the R_{AA} results with the ALICE data for the centrality classes 30%–50%, 50%–70% and 70%–90% [1].

ment in the more peripheral region, while scenarios 2 and 3 are more suitable for more central collisions where the b-dependence is more relevant. More details about each scenario can be found in [16].

6. Summary

In this work, the estimates for the rapidity distribution and nuclear modification factor were presented for the J/ψ production in the centrality classes 30%–50%, 50%–70% and 70%–90%. The ALICE measurements were compared with our estimates, obtained from three different approaches. In the simplest approach (scenario 1), better agreement was obtained with the data only in the more peripheral region, where there is a considerable uncertainty. For the more consistent approach (scenario 3), the result overestimates in the more peripheral region, however, it agrees better with the data in more central region, where the color dipole formalism is more intensely tested. Although it is not yet possible to confirm that the exclusive photoproduction is fully responsible for the J/ψ excess observed in ALICE, there are indications that it produces a considerable part of the effect.

REFERENCES

[1] J. Adam *et al.* [ALICE Collaboration], *Phys. Rev. Lett.* **116**, 222301 (2016).
[2] B. Abelev *et al.* [ALICE Collaboration], *Phys. Lett. B* **734**, 314 (2014).
[3] B. Abelev *et al.* [ALICE Collaboration], *Phys. Rev. C* **88**, 044909 (2013).
[4] M.K. Gawenda, A. Szczurek, *Phys. Rev. C* **93**, 044912 (2016).
[5] F. Krauss, M. Greiner, G. Soff, *Prog. Part. Nucl. Phys.* **39**, 503 (1997).
[6] K.T.R. Davies, J.R. Nix, *Phys. Rev. C* **14**, 1977 (1976).
[7] A.L. Ayala Filho, M.B. Gay Ducati, E.M. Levin, *Nucl. Phys. B* **493**, 305 (1997).
[8] A.L. Ayala Filho, M.B. Gay Ducati, E.M. Levin, *Nucl. Phys. B* **511**, 355 (1998).
[9] A.L. Ayala Filho, M.B. Gay Ducati, E.M. Levin, *Eur. Phys. J. C* **8**, 115 (1999).
[10] M.B. Gay Ducati, F. Kopp, M.V.T. Machado, S. Martins, *Phys. Rev. D* **94**, 094023 (2016).
[11] H. Kowalski, L. Motyka, G. Watt, *Phys. Rev. D* **74**, 074016 (2006).
[12] V.N. Gribov, *Sov. Phys. JETP* **29**, 483 (1969).
[13] V.N. Gribov, *Sov. Phys. JETP* **30**, 709 (1970).
[14] N. Armesto, *Eur. Phys. J. C* **26**, 35 (2002).
[15] M.B. Gay Ducati, S. Martins, *Phys. Rev. D* **96**, 056014 (2017).
[16] M.B. Gay Ducati, S. Martins, *Phys. Rev. D* **97**, 116013 (2018).